ORIGINAL PAPER

Photopolymerized silver-containing conducting polymer films. Part II. Physico-chemical characterization and mechanism of photopolymerization process

Dalibor Hodko · Maria Gamboa-Aldeco · Oliver J. Murphy

Abstract Physico-chemical and mechanical characterizations of nanophase silver-containing polypyrrole films prepared using a new photopolymerization process were performed. In general, the recorded physical, chemical, and mechanical data characteristic of these films was similar to corresponding literature data obtained from electropolymerized or chemically polymerized polypyrrole. However, photopolymerized polypyrrole films possessed an unusually high anion-to-monomer ratio of 0.8:1. Also, the photopolymerized material contained silver nanoparticles, having diameters of 2 μm or less, uniformly distributed throughout the polymer matrix. While the photopolymerization mechanism is complex, it is suggested that a pyrrole–silver cation complex is most likely the key component involved in the photopolymerization initiation step.

Keywords Electronically conducting polymers ·
Photopolymerization · Thin and thick polymer films ·
Spectroscopic techniques · Silver grains

M. Gamboa-Aldeco · O. J. Murphy (✉)
Lynntech, Inc.,
7610 Eastmark Drive,
College Station, TX 77840, USA
e-mail: oliver.murphy@lynntech.com

D. Hodko
Nanogen, Inc.,
10398 Pacific Center Court,
San Diego, CA 92121, USA

Introduction

π-conjugated conducting polymers have been the subject of both extensive and intensive fundamental and applied investigations since "doped" polyacetylene, polypyrrole, polyaniline, and polythiophene were found to be electronically conducting [1–3]. Electronic conductivity in these and related polymers arises from a delocalized π–electron band associated with polymer backbone structures containing alternating single and double bonds in either linear chains or aromatic ring structures [4]. In the oxidized state, positive charges along conjugated polymer chains are charge-balanced by incorporated, or "doped", anions while in the reduced form anions exit the polymer structures yielding "undoped" electrically insulating (neutral) materials [5]. Anions which are intercalated are those present in solutions during growth of the polymer films or powders. Insertion of anions into, and withdrawal of anions from, conducting polymer films can be conveniently investigated at conducting polymer film/electrolyte solution interfaces on ramping up and down the electrode potential applied to conducting polymer films between appropriate electrode potential limits in electrochemical cells [6]. Concomitant with the insertion and withdrawal of anions at polymer/electrolyte interfaces is the egress and ingress of electrons taking place at polymer/metal substrate interfaces. Intrinsically, electronically conducting polymer films undergo oxidation–reduction processes associated with anion "doping"–"dedoping" phenomena giving rise to electronic conductivities covering a broad range of the order of 10^{-15} S cm^{-1} to 10^5 S cm^{-1} [7].

Polypyrrole is a particularly attractive π-conjugated conducting polymer because it is highly conductive in the "doped" state, incorporates a broad range of anions, and possesses satisfactory environmental stability [8, 9]. The

polymer consists of a single phase comprising rigid and flat positively charged polymer chains, "dopant" anions for charge neutrality, and solvent molecules. The polymer chains are themselves made up of planar arrays of monomer units joined by α–α bonds and with some α–β and β–β cross linkages [10, 11]. Strong attractive forces between the positive charges on the polymer chains and the negative charges on the anions allows separation lengths between them of only a few Angstroms in the charged state of the polymer [12]. The experimental conditions for polymer deposition, e.g., electrolyte type and concentration, electrode potential, solution pH, and temperature, greatly influence the resulting properties of conducting polymer films [13–15]. An important property is the amount of anion "doping", or insertion; this is normally in the range 0.25–0.33, that is, every third or fourth pyrrole monomer formally has an excess positive charge [16]. However, the mechanism of electropolymerization, considered to involve a surface phase formed by two-dimensional nucleation and growth, followed by gradual densification [17, 18], is not completely understood. Electrodeposited polypyrrole films are highly coherent, very dense [1.37–1.58 g cm^{-3}], and strongly adherent to most metal or semiconductor substrates [10, 19, 20].

Polypyrrole has attracted considerable interest in applications including batteries [21, 22], electrochromic displays [23], corrosion prevention [24, 25], and through-hole plating in printed circuit boards [26]. However, most of the π-conjugated conducting polymers, including polypyrrole, are synthesized at present by either electrochemical or chemical processes [27, 28] which have limitations and drawbacks with regard to preparing these materials on a large scale as films or coatings on conducting and non-conducting substrates. To overcome this situation, a process for depositing conducting polymer thin and thick films having excellent adherence and precise control over the placement of the films on various substrates is urgently needed [29–31] in order for the full exploitation of these materials, in particular in electronic devices, to be realized.

A new photopolymerization process for the deposition of thin or thick nanophase silver-containing conducting polymer films on various substrates was outlined in Part I. The process was optimized based on the: choice of photoinitiator; identity of electron acceptor; nature of the "doping" anion; and light intensity. The developed photopolymerization process is at least 20 times faster than the corresponding electropolymerization process for the deposition of conducting polymer films having the same thickness and does not require a conducting substrate for deposition to take place. Polypyrrole films were readily photopolymerized on metal, ceramic, glass, Teflon®, Mylar®, and polystyrene substrates. An advantage of the photopolymerization process is that it allows mechanical properties of conducting polymer films to be optimized by incorporating various foreign molecular species, such as co-monomers, flexibilizers, and stabilizers, into photopolymerizable formulations. This opens up new possibilities for their application in fields where use of the electropolymerization or chemical polymerization processes are not possible. Physico-chemical and mechanical characterizations of silver-containing photopolymerized polypyrrole films were carried out and are described in this paper. The results obtained show that photopolymerized films have properties similar to those of electropolymerized or chemically prepared films. An attempt at understanding the mechanism of the photopolymerization process in the case of pyrrole is also outlined.

Experimental equipment, procedures, and methods

Apparatus used and method employed for photopolymerizing conducting polymer films The equipment required, and the procedures adopted, for the photopolymerization of black-colored, silver-containing polypyrrole films on various conducting, and non-conducting, substrates exposed to the ambient air were described in Part I. Polypyrrole films were prepared from its monomer, pyrrole, which was freshly distilled under vacuum prior to use. When required, polymer films were removed from metal or glass substrates using a sharp scalpel.

Elemental analysis Weight percents of C, H, N, O, P, Fe, F, and Ag in photopolymerized polypyrrole films were determined by Galbraith Laboratories, Knoxville, Tennessee.

Thermogravimetric analysis Thermogravimetric analysis (TGA) weight loss profiles were recorded on a Perkin-Elmer System 7 analyzer at Broutman, Chicago, Illinois. Portions of polypyrrole films, weighing about 10 mg were heated in a platinum boat from 30 °C–1,000 °C in an air atmosphere, using heating rates of 20 °C and 5 °C per minute.

Differential scanning calorimetry Differential scanning calorimetry (DSC) analyses were performed by Broutman on a Perkin-Elmer System 7 calorimeter, the performance of which was first checked using a piece of indium metal. Polypyrrole samples, weighing approximately 3.8 mg, were heated from −10 °C to 480 °C in a nitrogen atmosphere, using a heating rate of 10 °C per minute. The computerized system was used to subtract the empty reference aluminum pan thermogram from that of the sample plus pan.

Scanning electron microscopy and energy dispersive spectroscopy Morphologies of the outer and fractured surfaces of photopolymerized (and electropolymerized) polypyrrole films were viewed at various magnifications, using a JEOL, model 6400, scanning electron microscope (SEM) (Surface Science Center, Texas A&M University, College Station, Texas) and the elemental contents of the films were determined, using a Tracor Northern energy dispersive spectrometer microanalysis system attached to the SEM.

Infrared spectra Transmission infrared spectra of pyrrole monomer and photopolymerized polypyrrole were recorded through the microscope accessory of a Fourier transform infrared (FTIR) spectrometer (Nicolet model 2OSXB FTIR with a Spectra-Scope microscope). A 60-μm thick intact photopolymerized polypyrrole film segment was used.

UV/VIS absorption spectroscopy The UV/VIS absorption spectrum was recorded using a very thin, semitransparent polypyrrole film photopolymerized on a fused silica plate ($1 \times 2.5 \times 0.1$ cm). The film was obtained on spreading a thin layer of a photopolymerizable formulation by pressing and drawing a microscope slide along the quartz plate.

^{13}C MAS NMR A carbon thirteen, magic angle spinning, nuclear magnetic resonance spectrum of photopolymerized polypyrrole was obtained by Spectral Data Services, Champaign, Illinois, using a 270 MHz NMR spectrometer.

X-ray diffraction The crystallographic structures of photopolymerized polypyrrole films were obtained using an X-ray diffraction (XRD) spectrometer (Texas A&M University, College Station, Texas). Rigaku D-maxB or a Scintag PAD-V diffractometers were employed, using CuK_{α} radiation.

Thermomechanical analysis Thermomechanical analysis (TMA) of a photopolymerized polypyrrole film was carried out using a Perkin-Elmer Series 7 analyzer (Broutman). The performance of the expansion probe was first checked, using a piece of indium metal. The polypyrrole sample was heated from -123 °C to $+385$ °C in a helium atmosphere, using a heating rate of 10 °C per minute. Sample expansion (or contraction) was measured by means of the expansion probe.

The flexibility of polypyrrole films was determined qualitatively by bending film segments after removing them from the substrates on which they were deposited. Where photopolymerization resulted in very adherent films, flexibility was checked by bending the films together with the substrate (e.g., Teflon® or polystyrene)

Results and discussion

Subtle changes to the experimental conditions used to photopolymerize conducting polymer films gave rise to significant changes in the electronic conductivity and electrochemical activity of the polymer materials obtained, cf., Part I. To fully understand these, a series of investigations using chemical, thermal, and mechanical analysis techniques, together with various spectroscopic methods, were undertaken, aimed at exploring the effects of synthetic conditions on the physical, chemical, and mechanical properties of silver-containing polypyrrole films, as well as to gain an understanding of the mechanism of the photopolymerization process.

Elemental analyses Elemental analysis for a photopolymerized polypyrrole film derived from a photopolymerizable formulation containing only pyrrole and silver nitrate in the molar ratio of 16:1 pyrrole–silver nitrate was obtained initially. Normalizing to four carbon atoms yielded a molecular formula of $[C_4H_{4.10}N_{0.90}(AgNO_3)_{0.44}(H_2O)_{0.14}]_n$. Also, elemental analysis for a polypyrrole film derived from a formulation consisting of pyrrole–silver nitrate in the molar ratio of 8:1 and 3 wt.% Irgacure 261 as photoinitiator gave rise to a molecular formula of $[C_4H_{5.05}N_{0.83}(AgNO_3)_{0.80}(H_2O)_{0.12}(Initiator)_{0.015}]_n$, again on normalizing to four carbon atoms. The lower molar ratio of pyrrole–silver nitrate gave rise to a very high anion–monomer ratio of 0.8. The achievement of such a high level of "dopant" concentration has not been reported previously for electropolymerized or chemically polymerized polypyrrole.

Normally, the anion "doping" level for heterocyclic conducting polymers, defined as the incorporated anion–monomer ratio, is in the range of 0.20–0.40 [11, 32, 33]. For a "doping" level off 0.33, every third monomer in a polymer chain is positively charged and the resulting coulombic repulsion is weak, hence, conducting polymers possess high electrochemical stability. As the anion "doping" level reaches 0.5, which requires every second monomer to be positively charged, it might be expected that increasing coulombic repulsion would give rise to polymer instability [16]. However, it has been reported that for polypyrrole electrodeposited on platinum and iron anodes from aqueous KNO_3 solutions, strongly adhering, smooth and stable polymer layers were obtained having "doping" levels of 0.50 and 0.52, respectively [32]. Again, using NO_3^- as the "dopant" anion in the present investigation, a doping level of 0.80 for photopolymerized polypyrrole films on platinum was obtained. On subjecting the latter polymer films to multiple electrochemical oxidation/reduction cycles in acid solution, their stability was found to be good. A concern with trying to achieve high "doping" levels in electronically conducting polymers, at least for

those prepared electrochemically, is that the magnitude of the electrode potential required may result in overoxidation effects [16]. With the present photopolymerization process, this does not appear to be a problem.

A hydrogen content higher than ideal for photopolymerized polypyrrole (four or five found versus three theoretical) indicates: (1) that the polymer may not simply be a linear chain of α–α bonded pyrrole units but may also contain some saturated pyrrolidine units or partially saturated units and/or (2) the pyrrole nitrogen atoms are protonated. Excess hydrogen has also been observed in the case of chemically prepared polypyrrole materials [19, 34]. It is interesting to note that no excess oxygen was found for the photopolymerized polypyrrole films. The elemental analyses account for 94–99% of the polymer materials analyzed and are consistent with polymerized pyrrole units, along with incorporated charge counter balancing anions (NO_3^-) as well as the electron acceptor (Ag^+) and photo-initiator (Irgacure 261), where appropriate.

Thermogravimetric analysis and differential scanning calorimetry Thermogravimetric analysis and differential scanning calorimetry allow a determination of the thermal characteristics and stabilities of materials to be made. The weight percent of volatile species that are evolved from materials as a result of being heated and the related endothermic and exothermic processes can be readily observed. A TGA profile for a photopolymerized polypyrrole film is presented in Fig. 1. A weight loss of 2% occurs between room temperature and 150 °C. This is most likely associated with the evolution of water vapor from this hygroscopic material [35]. The magnitude of the hydration energy on fully hydrating "dopant" anions and positively charged monomer moieties in polymer backbones, provides an extremely strong driving force for the uptake of water molecules by intrinsically, electronically

Fig. 2 Differential scanning calorimetry trace for a photopolymerized polypyrrole film derived from a photopolymerizable formulation containing pyrrole–silver nitrate=8:1 and 3 wt.% Irgacure 261

conducting polymers. Slightly higher weight losses over this temperature range have been reported for electrochemically prepared polypyrrole materials [35, 36]. Volatilization of water over this temperature range is supported by the endothermic peaks, centered at approximately 80 °C (physically adsorbed water) and approximately 150 °C (chemisorbed water) in the DSC trace shown in Fig. 2.

A weight loss of about 8 wt.% occurs over the temperature range 175–225 °C, which may be associated with the degradation of incorporated nitrate anions. A significant weight loss arising from the thermally induced degradation of the polymer occurs only at temperatures greater than 225 °C. The broad exothermic peak at 225 °C in the differential scanning calorimetry profile, cf., Fig. 2, corresponds to the thermal decomposition temperature of the polypyrrole material and is in agreement with the rapid weight loss, shown in the TGA profile cf., Fig. 1. The residue remaining after the decomposition of photopolymerized polypyrrole, of the order of 50 wt.%, is most likely due to a silver-containing compound but not silver oxides, since they decompose at much lower temperatures [37]. The char yield for a 90/10 pyrrole/ethylaniline copolymer after being heated to 500 °C in air was 34% [38].

Thermomechanical analysis The degree of flexibility of a photopolymerized polypyrrole film was determined qualitatively by bending film segments after removing them from their substrates. Polymer films displayed a low degree of flexibility in that they easily fractured on being bent through an angle of 90°. This is in keeping with the relatively poor mechanical properties demonstrated by polypyrrole films in general, except those electrodeposited from acetonitrile solutions [35]. A thermomechanical analysis profile for a photopolymerized polypyrrole film is presented in Fig. 3. The polymer sample did not undergo much dimensional change until a temperature of 30–40 °C
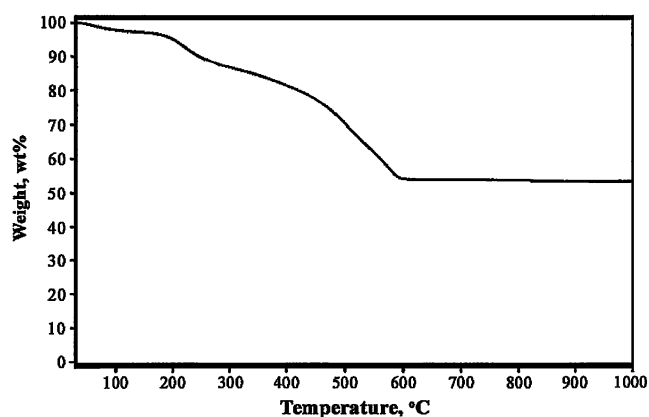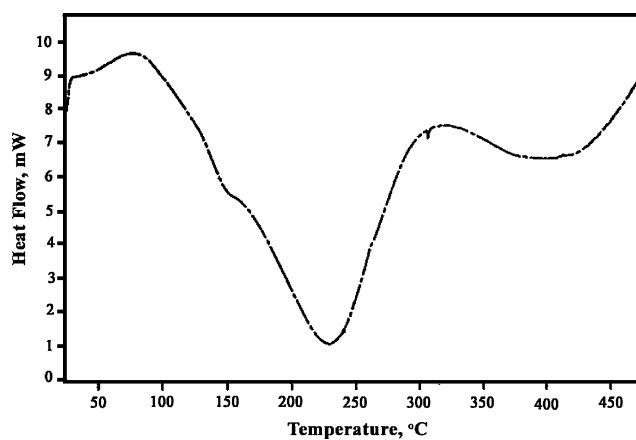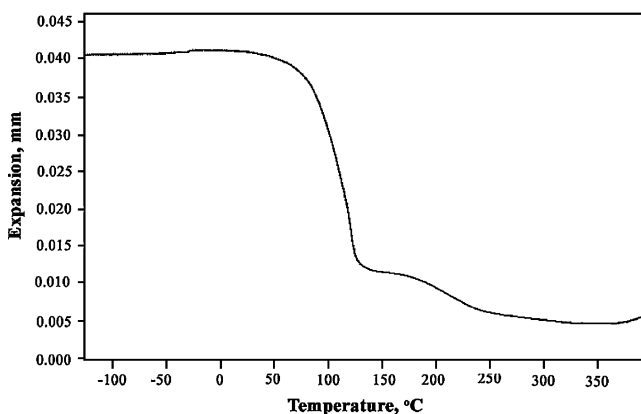

Fig. 1 Thermogravimetric analysis profile for a photopolymerized polypyrrole film derived from a photopolymerizable formulation containing pyrrole–silver nitrate=8:1 and 3 wt.% Irgacure 261

Fig. 3 Thermomechanical analysis profile for a photopolymerized polypyrrole film derived from a photopolymerizable formulation containing pyrrole–silver nitrate=8:1 and 3 wt.% Irgacure 261

was reached. At these and higher temperatures, it appeared as if the film began to contract. This apparent contraction is most likely due to softening of the polypyrrole matrix, resulting in penetration of the expansion probe in through the polymer film. From −110 °C to +27 °C, the expansion coefficient for the photochemically prepared polypyrrole film was calculated to be 25.7×10^{-6}/°C. For a polypyrrole film electrodeposited from an aqueous solution containing p-toluenesulfonate anions, the expansion coefficient was found to be 54.7×10^{-6}/°C in this investigation. Examination of the linear expansion region, cf., Fig. 3, shows that photopolymerized polypyrrole does not give rise to a glass transition temperature, T_g, which has been pointed out previously for conducting polypyrrole materials [39]. It has been noted that the moisture contained within polypyrrole films acts as a plasticizer, and its removal, or loss, leads to substantial embrittlement [36].

Infrared transmission spectra The infrared transmission spectra of pyrrole and a free-standing film of photopolymerized polypyrrole are given in Fig. 4. Compared to pyrrole, the bands for the polypyrrole material are broad, indicative of an amorphous structure for this material. The region of 500–1,800 cm^{-1} in the spectrum of the polypyrrole material, cf., Fig. 4b, contains bands consistent with the presence of the pyrrole moiety, cf., Fig. 4a. The spectrum for photopolymerized polypyrrole shows a broad featureless decrease in transmission from 1,800 cm^{-1} to 3,400 cm^{-1} which is characteristic of conducting polymers in their oxidized state [32, 35]. This broad feature has been attributed to the presence of free charge carriers on the conducting polypyrrole backbone [40] and to electronic transitions from the valence band to electronic states in the bandgap region [41]. The sharp and very strong band at 735 cm^{-1} observed for pyrrole (Fig. 4a), assigned to C–H out-of-plane bending in the pyrrole ring, is considerably

reduced in intensity for the polypyrrole material (Fig. 4b). This is a strong indication that the material has the structure characteristic of polypyrrole [42].

Infrared band positions from the two spectra presented in Fig. 4, along with characteristic bands for silver nitrate, are given in Table 1. Examination of the data presented in the table shows that the vibrational modes of the pyrrole monomer are conserved in the polymer to a large extent. However, polymerization modifies band intensities and shifts them to lower wavenumbers. Also, from Table 1, overlapping and/or new bands due to the presence of incorporated nitrate anions in the polypyrrole matrix can be distinguished.

UV/VIS absorption spectroscopy A UV/VIS spectrum was obtained for a very thin polypyrrole film (pyrrole–AgNO$_3$= 8:1, 3 wt.% Irgacure 261) photopolymerized on a quartz substrate. The resulting absorption spectrum is shown in Fig. 5. A small shoulder can be seen at about 270 nm and a
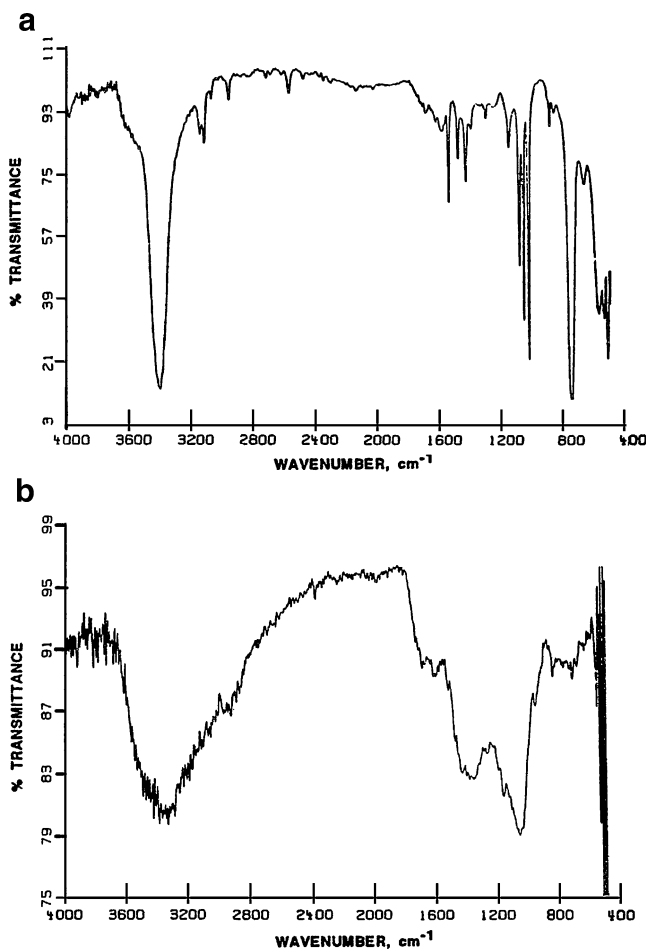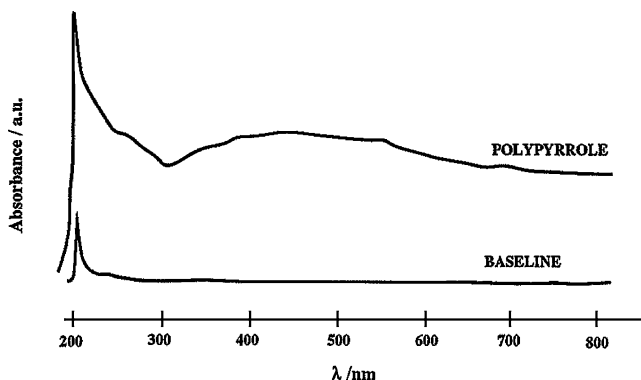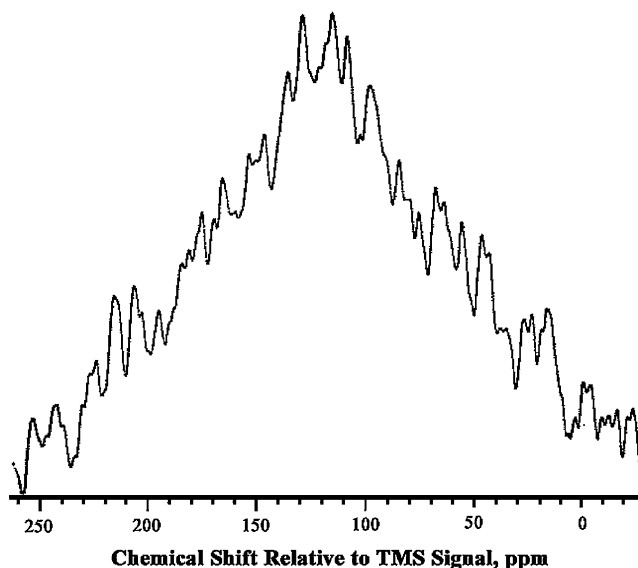

Fig. 4 Fourier transform infrared transmission spectra of **a** pyrrole and **b** a free-standing film of photopolymerized polypyrrole derived from a photopolymerizable formulation containing pyrrole–silver nitrate=8:1 and 3 wt.% Irgacure 261

Table 1 Infrared band positions (cm^{-1}) for pyrrole, photopolymerized polypyrrole, and silver nitrate

Vibration mode	Pyrrole	Photopolymerized polypyrrole	Silver nitrate
NH stretching	3,390	3,340	
CH stretching	3,120	–	
CH stretching	3,100	–	
	2,940	2,920	
	2,550	–	
	1,670	1,660	
	1,575	1,580	
	1,525	1,500	
Ring stretching	1,465	1,460	
Ring stretching	1,415	1,410	
Ring stretching	1,380	1,375–1,340	1,340 (VS)
Ring stretching	1,280	1,260	
	–		
NH in-plane	1,140	1,160	
	–	1,050	1,040 (W)
CH in- and out-of-plane	1,070	1,030	
CH in- and out-of-plane	1,050	–	
CH in- and out-of-plane	1,015	950	
	–	–	
	865	–	
	–	825	805 (S)
	735	735	
	–	700	725 (M)
	–	–	
	655	–	
	560	540	

M Medium intensity, *W* weak intensity, *S* strong intensity, *VS* very strong intensity

broad maximum at about 450 nm. The latter has been identified as a characteristic peak of oxidized polypyrrole [43–45] and has been attributed to charge transitions between the valence band and antibipolaron energy states within the bandgap of polypyrrole [43, 46]. The bipolaron band corresponds to a peak normally observed at 900 nm


Fig. 5 UV/VIS absorption spectrum of photopolymerized polypyrrole derived from a photopolymerizable formulation containing pyrrole–$AgNO_3$=8:1 and 3 wt.% Irgacure 261

Fig. 6 ^{13}C NMR spectrum of photopolymerized polypyrrole derived from a photopolymerizable formulation containing pyrrole–silver nitrate=8:1 and 3 wt.% Irgacure 261

[47]. The sum of the bipolaron and antibipolaron energy levels is approximately equal to the bandgap [46].

^{13}C MAS NMR ^{13}C NMR spectroscopy is a powerful technique widely used for determining the structures of solubilized polymers. The broadening of NMR spectra derived from solids can be considerably reduced by spinning the solid sample about an axis, inclined at an angle of 54.7°, known as the "Magic Angle" [39]. A ^{13}C MAS NMR spectrum of photopolymerized polypyrrole that had been exposed to the air is presented in Fig. 6. However, even under MAS conditions, only a very broad, almost symmetric peak was obtained, having a peak maximum at 125 ppm downfield from tetramethylsilane. Similar solid state NMR was reported earlier [48] and was interpreted in terms of the removal of π-electrons, leading to the formation of cations within the polypyrrole matrix. The ^{13}C MAS NMR spectrum for photopolymerized polypyrrole is consistent with the presence of the pyrrole monomer and the downfield shift with respect to the α-carbons of pyrrole (α-carbons for pyrrole give a peak at 117 ppm [49]) is indicative of α–α linkages in the photopolymerized polymer material.

Scanning electron micrographs and energy dispersive spectroscopy Scanning electron micrographs of fracture surfaces of thick photopolymerized (70 μm) and electropolymerized (67 μm) polypyrrole films, together with their corresponding energy dispersive spectrographs, are shown in Fig. 7. It can be seen from Fig. 7a that electrochemically prepared polypyrrole is dense, non-fibrillar, and volume-

Fig. 7 Scanning electron micrographs of the cross-sections of polypyrrole films **a** for electrochemically and **b** for photochemically prepared polypyrrole films—the electropolymerized film was deposited from an aqueous solution containing 0.1 M C$_4$H$_4$NH and 0.1 M CH$_3$(C$_6$H$_4$)SO$_3$Na as described in Ref. [50]—the photopolymerized polypyrrole film was derived from a photopolymerizable formulation containing pyrrole–silver nitrate=8:1 and 3 wt.% Irgacure 261—corresponding energy dispersive spectrographs are shown in **c** and **d**, respectively
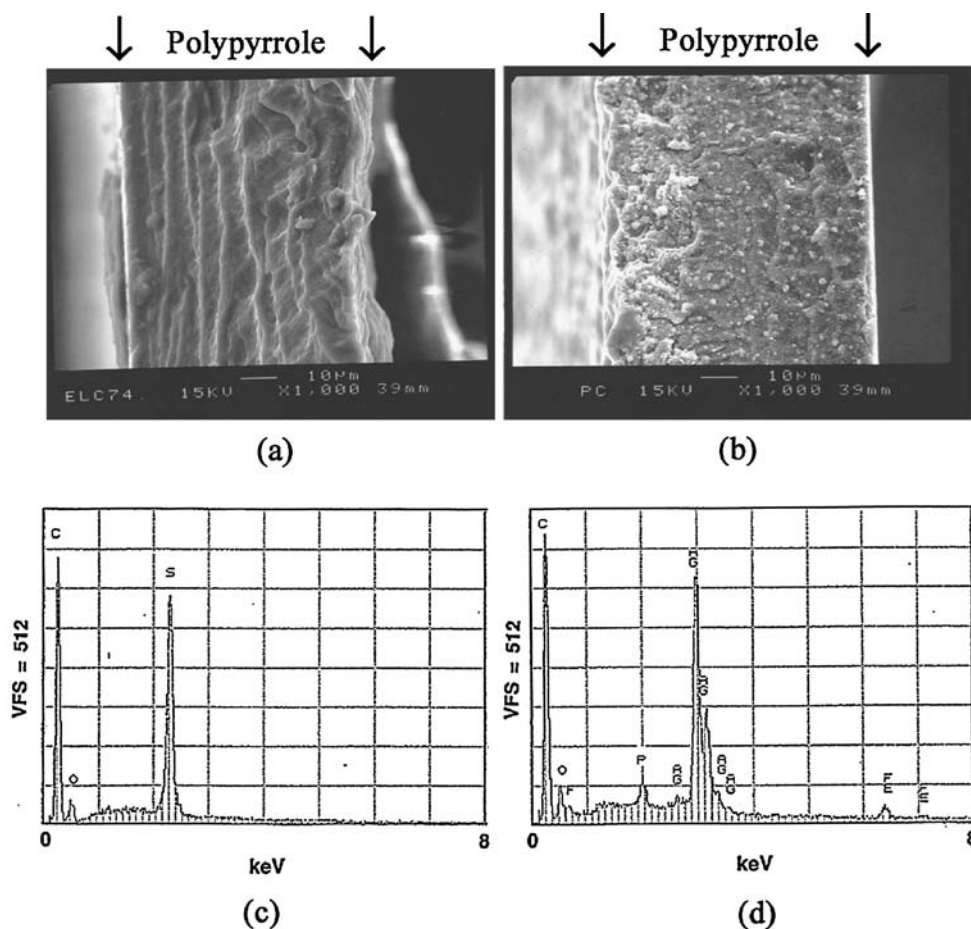

filling [35, 51]. The photopolymerized material (cf., Fig. 7b) is compact, but more open-structured and contains some voids.

The major elements present in the surface regions of the films were identified by energy dispersive spectroscopy. Spectrographs are presented in Fig. 7c,d for each film type. Electrochemically prepared films consisted mainly of C, S, and O, the latter two elements originating from the "dopant" tosylate anions. The major elemental constituents of photochemically prepared films were C and Ag, and small amounts of Fe, P, and F, originating from the photoinitiator, Irgacure 261, present in the amount of 3 wt.%. Small "white" grains were visible on the fractured surface of the photopolymerized film (cf., Fig. 7b). On focusing the X-ray beam on these "white" grains, energy dispersive spectroscopy revealed silver as the only constituent of these grains. Various physical and chemical processes have been investigated with the aim of incorporating silver nanoparticles into polymer films [52]; however achieving uniform distributions in polymer matrices has proven difficult since suspensions or dispersions of silver nanopoarticles are prone to aggregate [53]. The photopolymerization process described here provides a unique approach for bringing about a uniform distribution of silver nanoparticles throughout the thickness of conducting polymer films.

Scanning electron micrographs at two magnifications of the outer surfaces of electropolymerized and photopolymerized polypyrrole films are presented in Fig. 8. For electrochemically prepared polypyrrole (cf., Fig. 8a,c), nodular or "cauliflower" structures can be clearly seen that are consistent with a nucleation/dendritic film growth mechanism [51, 54]. This surface topology is frequently observed for electrochemically prepared polypyrrole materials. In contrast, the surface topography for photopolymerized polypyrrole films is rather featureless, being smooth and flat (cf., Fig. 8b,d). As observed in the micrograph of the fractured surface of photopolymerized polypyrrole (cf., Fig. 7b) a large number of evenly distributed silver grains of surprisingly uniform size can be seen also on its outer surface. In the higher magnification electron micrograph (cf., Fig. 8d) the bright, reflective, multifaceted silver particles were determined to be 2 μm or less in average diameter. For both polypyrrole film types, the surfaces adhering to the substrates were smooth, shiny, and featureless.

Fig. 8 Scanning electron micrographs at two magnifications of the outer surfaces of polypyrrole films: **a** and **c** electrochemically deposited; **b** and **d** photochemically polymerized—the electropolymerized material was deposited from an aqueous solution containing 0.1 M C_4H_4NH and 0.1 M $CH_3(C_6H_4)SO_3Na$ as described in Ref. [50]—the photopolymerized polypyrrole film was derived from a photopolymerizable formulation containing pyrrole–silver nitrate=8:1 and 3 wt.% Irgacure 261
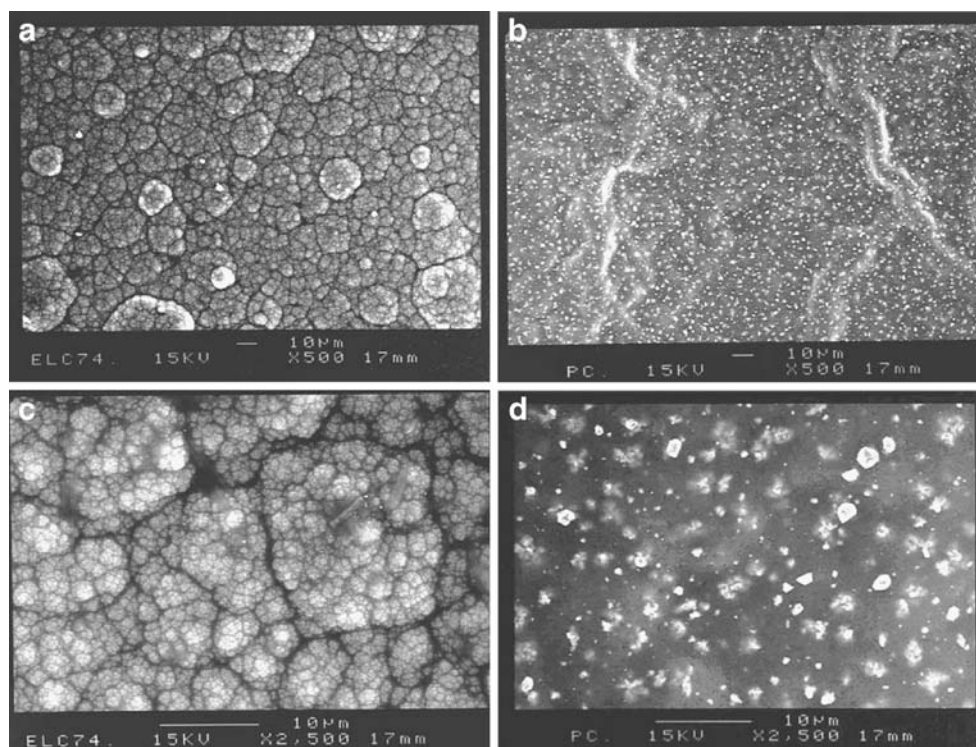
X-ray diffraction To determine the structure of photopolymerized polypyrrole and the degree of crystallinity of the silver grains present in the films, X-ray diffraction spectroscopy was performed on samples which showed the highest electrical conductivity. X-ray scattering intensity versus 2θ for a polypyrrole sample prepared using pyrrole–electron acceptor=8:1 and containing 3 wt.% of Irgacure 261 photoinitiator is presented in Fig. 9. The polymer is essentially amorphous to X-rays for angles of 2θ between 5 and 35° (cf,. Fig. 9a). A single broad maximum corresponding to a d-spacing of 4.0774 Å (2θ=21.78°) can be seen indicating weak ordering parallel to the polymer chains. Similar XRD profiles were obtained for the related amorphous electronically conducting polymer, polyaniline [56, 57].

Electronically conducting polypyrrole, prepared chemically or electrochemically, normally gives rise to a broad distribution of scattered X-ray intensity around a high angle of 2θ in the range 20–25°, that is for a d-spacing of 4.436–3.559 Å, respectively [35, 50, 54, 55]. In some cases, this broad distribution of X-ray intensity is comprised of two poorly resolved peaks [35]. For electropolymerized polypyrrole "doped" with tosylate anions, a first peak maximum is observed at a d-spacing of 3.5 Å which was assigned to scattering from pyrrole chains at interplanar spacings close to the van der Waals distance for aromatic groups [35]. A second peak maximum at a d-spacing of 4.13 Å was considered to be due to pyrrole–tosylate (or intertosylate) scattering, as the displacement due to the presence of the large tosylate anion would increase the interplanar spacing

of pyrrole chains over that of a tosylate-free polypyrrole chain environment.

A peak maximum at a d-spacing of 4.07 Å obtained for photopolymerized films is slightly higher than 3.55 Å observed for electropolymerized films. Possibly the packing of polypyrrole chains is somewhat expanded by the presence of silver grains. On recording the X-ray diffraction pattern at larger angles (cf., Fig. 9b), three distinct sharp peaks were observed at d-spacings of 2.359 Å (intensity of 100%), 2.044 Å (intensity approximately 40%) and 1.445 Å (intensity approximately 25%). The relative intensities and positions of these peaks precisely correspond to the reflections from the (111), (200), and (220) planes of metallic silver. The silver is preferentially oriented along the (111) plane. No peaks characteristic of silver nitrate or of the photoinitiator were observed, which, in the case of the photoinitiator, is probably due to the small amount present in the polymer matrix.

The average diameter for silver grains having sizes in the range 5–100 nm can be calculated from Scherrer's equation [58]:

$$D = K\lambda / \beta \mathrm{Cos}\theta$$

where K is the shape factor and is assigned the value of 1.0 when the shape of the particles is neither strictly spherical or cubic [58], λ is the X-ray wavelength and has the value of 0.15406 nm, for Cu Kα radiation, β is the peak broadening measured at half-height and expressed in radians, and D is the average diameter of the grains in nm. Using the peak at 2θ=64.48, yields a value for D=31 nm.
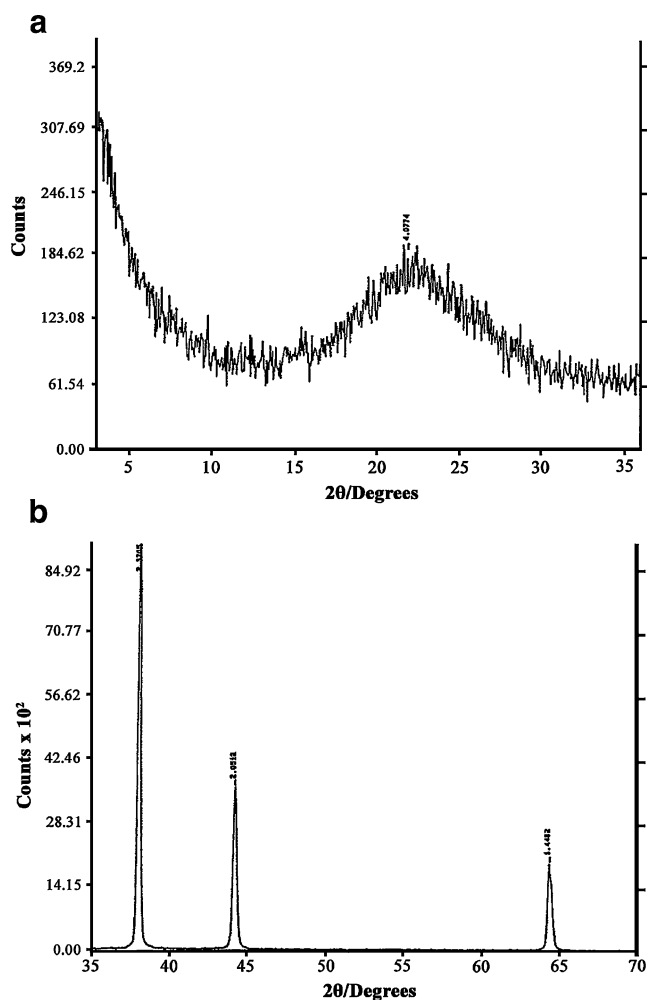
Fig. 9 X-ray diffraction pattern for photopolymerized polypyrrole: **a** range of 2θ corresponding to amorphous polypyrrole; **b** range of 2θ showing peaks characteristic of polycrystalline silver metal

Chemical stability of photopolymerized polypyrrole films

Samples of photopolymerized polypyrrole analyzed by X-ray diffraction were subjected to immersion in 1.0 M HNO_3 for 3 weeks, in order to determine their resistance to aggressive chemicals. Samples were kept immersed in the nitric acid solution for 24 h. At the end of each 24-h period, samples were removed from the acid solution, washed with nanopure water and re-immersed in fresh acid solution. The nitric acid solutions were collected and analyzed for silver by the ICP method.

An X-ray diffraction pattern for a photopolymerized polypyrrole sample after leaching silver in 1.0 M HNO_3 is shown in Fig. 10. The d-spacing obtained from the broad peak assigned to scattering from pyrrole rings, changed from 4.07 Å (cf. Fig. 9a) to 3.72 Å (cf. Fig. 10a). This value is very close to 3.51 Å and 3.55 Å observed by Cvetko et al [54] and by Wynne and Street [35] for

electropolymerized polypyrrole films. However, two new broad peaks with d-spacings of 10.1 Å and 6.68 Å appeared. The peak at 6.68 Å probably originates from partial reordering of polypyrrole chains as a result of leaching silver. For electronically conducting polypyrrole "doped" with large anions, in particular large amphiphilic organic anions, a second distribution of scattered X-ray intensity is observed at a low angle of 2θ in the range 3–9°, that is, for d-spacings of 29.43–9.82 Å, respectively [35, 50, 55]. This secondary distribution has been attributed to short range order involving "dopant" anions [35, 50, 55]. For "dopant" nitrate anions, having an ionic radius in the range 1.65–1.89 Å [59, 60], the weak low angle peak at the d-spacing of 10.1 Å indicates that there is significantly less anion order in the photopolymerized polypyrrole material than in electropolymerized polypyrrole "doped" with long alkyl chain-containing sulfonates and sulfates, where intense low angle scattering yielded a linear relationship with the number of carbon atoms in the alkyl chain [55].

Examination of the polycrystalline silver peaks shows that the relative intensity ratio of the (111), (200), and (220) reflections changed from that characteristic of polycrystalline metallic silver, 100/45/25, to 35/45/25 (cf. Fig. 10b). Thus, it appears that dissolution of silver occurred preferentially at the exposed (111) planes of silver grains. A significant overall decrease in intensity of the peaks after leaching, indicates an approximately 80% reduction in the concentration of silver within the polypyrrole matrix. The predominance of the (200) peak indicates that the remaining silver exists in a well-crystallized form, but with preferred orientation, possibly determined by the orientation of the polypyrrole chains.

Silver metal grains in photopolymerized polypyrrole samples were leached into 10 ml aliquots of 1.0 M HNO_3, and the nitric acid solutions were then analyzed for silver by means of inductively coupled plasma spectroscopy. The silver content after three days of leaching was only 0.3 ppm/day, while it increased dramatically to 3,300 ppm/day after 6 days of leaching. After 21 days of leaching the concentration of silver found in the nitric acid solution had dropped to 10 ppm per day. A relatively long initiation period for the start of the leaching process (approximately 3–4 days) is indicative of the compact nature of the polymer material (cf, Figs. 7b and 8d).

Pyrrole–silver ion complex

Pyrrole is known to form complexes with silver salts [48]. Both chemical and thermal analysis showed the presence of two pyrrole monomers per Ag^+ cation. However, solution ^{1}H NMR of the pyrrole–silver salt complex indicated that it is largely dissociated in solution. A white polycrystalline
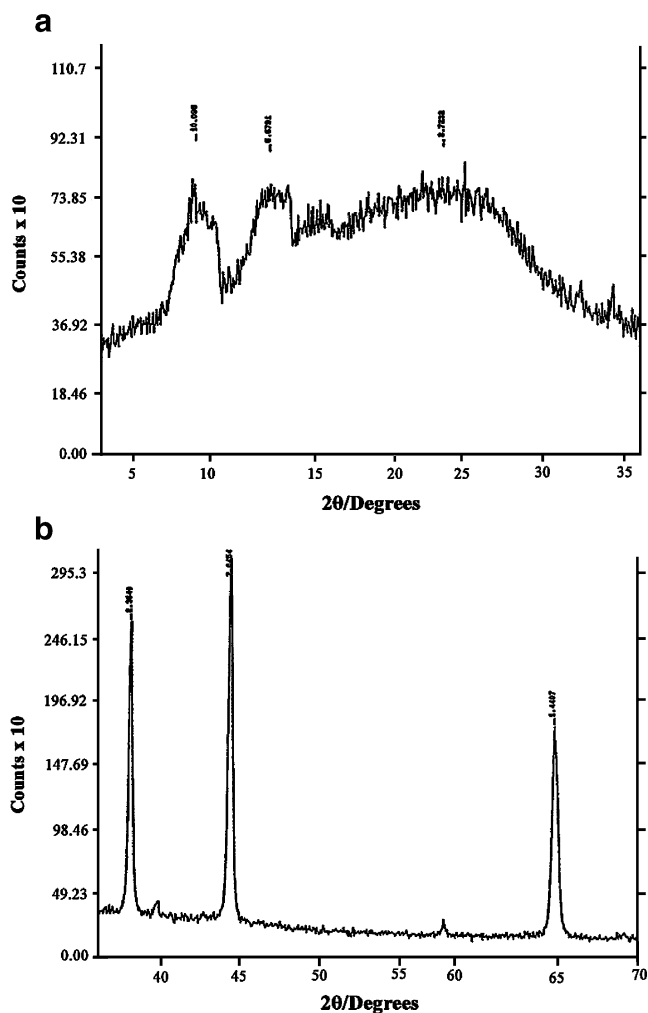
Fig. 10 X-ray diffraction pattern obtained from a photopolymerized polypyrrole sample after leaching silver in 1.0 M HNO$_3$: **a** 2θ range associated with polypyrrole; **b** 2θ range where silver metal is observed

involving the white powdered Ag–pyrrole complex occurred. It is clear that in this process Ag$^+$ cations served as electron acceptors on oxidizing pyrrole, and ClO$_4^-$ functioned as "dopant" anions in the dark polypyrrole material formed. In addition, amorphous material, likely to be polypyrrole, is present as evidenced by the broad maximum
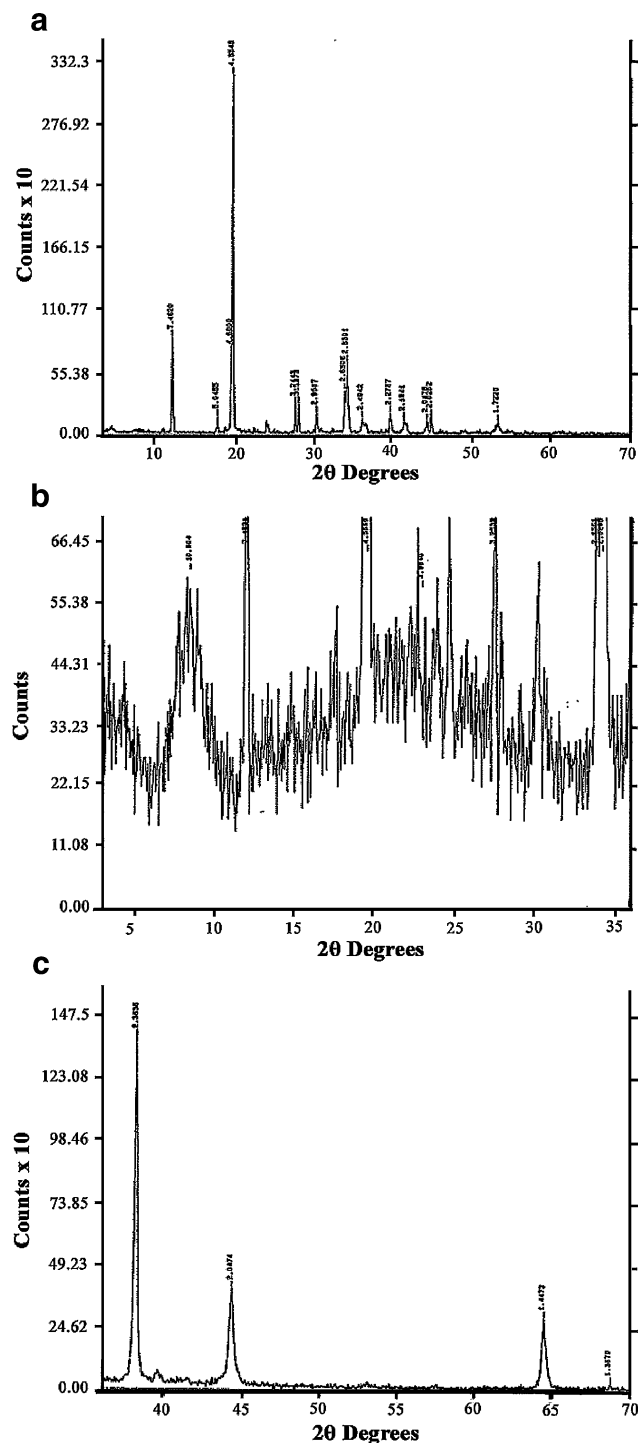
complex (AgPy$_2^+$ ClO$_4^-$) was precipitated by adding pyrrole to a toluene solution of silver perchlorate. It was observed that this complex when illuminated with UV light in air in the solid state turned black, suggesting that such a complex may be involved in the photopolymerization of polypyrrole films.

X-ray diffraction patterns of this dry, powdered Ag–pyrrole complex, before and after illumination (12 h), are shown in Fig. 11. The white-colored, non-illuminated Ag–pyrrole complex gave an X-ray diffraction pattern containing a number of sharp peaks, consistent with a single phase, highly polycrystalline material, and with no indications of silver metal present in the powder (cf., Fig. 11a). After illumination, a decrease in the intensity of the peaks characteristic of the white polycrystalline material occurred (cf., Fig. 11b,c). Three new peaks characteristic of polycrystalline metallic silver appeared (cf., Fig. 11c), clearly indicating that a solid state photochemical process

Fig. 11 X-ray diffraction patterns for silver–pyrrole complex: **a** no illumination; **b** and **c** after exposure to UV light

at a d-spacing of 3.9 Å (cf., Fig. 11b). The maximum at a d-spacing of 10.6 Å most likely arises from short range order involving the "dopant" ClO_4^- anions; this anion has an ionic radius of 2.26 Å [60]. These maxima are related to the maxima observed for silver leached photopolymerized polypyrrole films (cf., Fig. 10a).

Mechanism of photopolymerization of electronically conducting polymer films

Although the actual mechanism of the photopolymerization process used in this investigation is not completely understood, some aspects of the chemistry and photochemistry involved need to be addressed. Conducting polypyrrole films were prepared photochemically when pyrrole monomer, Ag^+ cations and NO_3^- anions were present in photopolymerizable formulations. Increased rates of photopolymerization with increasing photoinitiator concentrations in formulations, strongly suggests that the polymerization process taking place is photochemical in nature. It was found that the most efficient photoinitiators were cationic photoinitiators, indicating a cationic mechanism for the photopolymerization process.

Pyrrole monomer is slowly oxidized by Ag^+ cations. In comparison to Fe^{3+} and Cu^{2+} cations, Ag^+, has the highest standard reversible potential; standard potentials decrease in the order $Ag^+>Fe^{3+}>Cu^{2+}$ (0.800>0.771>0.153 V (SHE)). It is interesting to note that the rates of chemical polymerizations decrease in the order: $Fe^{3+}>Cu^{2+}>Ag^+$ [61]. This is in contrast to the electrochemical method where a cationic radical formed requires a high positive electrode potential. Typically 1.0 V (SHE) has to be applied in order for the polymerization reaction to occur. Although, Ag^+ has the highest standard reversible potential, yet its reaction rate with pyrrole is slow (1–2 days in the dark). It has been suggested that the observed differences in reaction rates follow the order of the K_h values of the hydrated metal cations: $Fe^{3+} <Ag^+<Cu^{2+}$ (pK_h=2.19, 6.90, 7.53, respectively) [61].

The increase in the polymerization rate under UV illumination may be influenced by several factors. Self-sensitized polymerization of pyrrole in the presence of sunlight is known to take place [62]. It was suggested that pyrrole monomers absorb light in the near UV region, giving rise to photoexcited pyrrole molecules, which are rapidly quenched by unexcited pyrrole molecules, giving both cationic and anionic pyrrole radicals [62]. The pyrrole cation radicals then react with pyrrole monomers in solution, forming dimers and oligomers which can absorb light at longer wavelengths, creating new radical centers for polymerization. Another plausible photoinitiation step may involve Ag^+ cations in a photoexcited state upon illumination of silver–pyrrole complexes with UV light, which become more reactive, thus increasing the rate of pyrrole oxidation and polymerization.

Irgacure 261 photoinitiator [η^6-benzene) (η^5-cyclopentadienyl)iron(II)-hexafluorophosphate] undergoes photolysis by dissociation of the uncharged aromatic ligand with formation of a coordinatively unsaturated iron (II) cation intermediate [63]. This reactive intermediate is known to coordinate with nucleophilic monomers. The photoactivity of Irgacure 261 is enhanced by oxidizing agents, including peroxides, which are believed to oxidize the iron (II) intermediate species to iron (III). The even more electrophilic iron (III) species is a more effective initiator for polymerization of nucleophilic monomers. It appears reasonable, that any photogenerated iron (II) intermediate (from Irgacure 261) is oxidized by Ag^+ to yield Ag^0 and that the iron (III) intermediate formed participates in the oxidative polymerization of pyrrole.

The fact that better quality photopolymerized polypyrrole films were obtained when NO_3^- was used in formulations, as compared to Ts^-, BF_4^-, ClO_4^-, and NO_2^- anions of silver salts, is intriguing. However, it should be noted that excellent deposits of electropolymerized polypyrrole were formed on active iron and platinum substrates in aqueous solution, only when NO_3^- anions were present, along with pyrrole monomers [32]. Because of the tendency of NO_3^- ions to yield radicals at an anode surface, it was speculated that such radicals could initiate radical-induced oxidative polymerization of pyrrole [32]. Such radical formation involving NO_3^- anions is much more favorable in non-aqueous systems, similar to those of the photopolymerizable formulations employed in the present investigation. It is possible that the nitrate anion plays a role in the photopolymerization of pyrrole, in addition to counter balancing the positive charge in the polypyrrole chains.

The process, or processes, taking place in the photopolymerizable formulations used in the present investigation are complex and probably involve the participation of at least the following four components: pyrrole monomer (or more likely pyrrole–Ag^+ complex); Ag^+ cations; NO_3^- anions; and photoinitiator. Since it has been demonstrated in this investigation that C_4H_4NH complexed with Ag^+ cations polymerize under UV illumination, it is probable that pyrrole undergoes complexation with silver cations and that this complex, which is likely to be more easily oxidized than non-complexed C_4H_4NH, is involved primarily in the polymerization initiation step.

Conclusions

The physical, chemical, and mechanical properties of silver-containing polypyrrole films laid down using a new

photopolymerization process were obtained using a plethora of spectroscopic and other materials characterization techniques. In general, the recorded physical, chemical, and mechanical data characteristic of photopolymerized, silver-containing polypyrrole was similar to corresponding data obtained from the literature for electropolymerized and chemically prepared materials.

A difference between the conducting polymer materials synthesized by the photopolymerization process and either the electrochemical, or chemical, process is the high anion-to-monomer ratio up to 0.80:1 for photopolymerized polypyrrole compared to 0.25–0.33:1 for electrochemically or chemically prepared polypyrrole. The ability to significantly enhance the anion "dopant" content of conducing polymers could give rise to the more effective use of these materials in a variety of applications. Also, the photopolymerized polypyrrole films have silver nanoparticles uniformly distributed throughout the depths of deposited films. The silver is in the form of polycrystalline grains having diameters of 2 μm, or less, and expose the major crystal planes. Most, if not all, of the silver can be dissolved out of photopolymerized polypyrrole matrices in acid solutions indicating the presence of micropores in these materials. The ability to uniformly incorporate silver nanoparticles into conducting polymer materials has long been sought after because such composites could have unique catalytic, optical, and sensing properties.

The photopolymerization process is complex and the photoinitiation step is still not completely understood. The process yields silver-containing polypyrrole material, even in the absence of a photoinitiator, so long as silver nitrate is included in the formulation. Since, it is known that pyrrole complexes with silver cations to give a silver–pyrrole complex consisting of two pyrrole monomers per silver cation and that this complex is likely to be more easily oxidized than non-complexed pyrrole, thus, it is probable that this complex is involved in the photopolymerization initiation step.

References

1. Shirakawa H (2001) Angew Chem Int Ed 40:2574 doi:10.1002/1521-3773(20010716)40:14<2574::AID-ANIE2574>3.0.CO;2-N
2. MacDiarmid AG (2001) Angew Chem Int Ed 40:2581 doi:10.1002/1521-3773(20010716)40:14<2581::AID-ANIE2581>3.0.CO;2-2
3. Heeger AJ (2001) Angew Chem Int Ed 40:2591 doi:10.1002/1521-3773(20010716)40:14<2591::AID-ANIE2591>3.0.CO;2-0
4. Epstein AF (2007) In: Mark JE (ed) Physical properties of polymer handbook, Chapter 46. 2nd edn. Springer, New York
5. Rehwald W, Kiess HG (1992) In: Keiss HG (ed) Conjugated conducting polymers, Chapter 3. Springer, Berlin
6. Inzelt G, Horanyi (1987) J Electronal Chem 230:257 doi:10.1016/0022-0728(87)80147-X
7. Bidan G (1992) Sensors Actuators B 6:45 doi:10.1016/0925-4005(92)80029-W
8. Inzelt G, Pineri M, Schultze JW, Vorotyntsev MA (2000) Electrochim Acta 45:2403 doi:10.1016/S0013-4686(00)00329-7
9. Wang LX, Li XG, Yang YL (2001) Reactive Funct Polymers 47:125 doi:10.1016/S1381-5148(00)00079-1
10. Billingham NC, Calvert PD (1989) Adv Polym Sci 90:1
11. Heinze J (1990) Top Curr Chem 152:1 doi:10.1007/BFb0034363
12. Inzelt G (2008) Conducting polymers:a new era in electrochemistry, Chapter 6. Springer, Berlin
13. Satoh M, Kaneto K, Yoshino K (1986) Synth Met 14:289 doi:10.1016/0379-6779(86)90042-1
14. Zhou M, Heinze J (1999) Electrochim Acta 44:1733 doi:10.1016/S0013-4686(98)00293-X
15. Park JH, Kim BW, Nho YC (2008) Electrochem Solid-State Lett 11:A68 doi:10.1149/1.2864979
16. Heinze J (1991) Synth Met 41–43:2805 doi:10.1016/0379-6779(91)91183-B
17. Asavapiriyanont S, Chandler GK, Gunawardena GA, Pletcher D (1984) J Electroanal Chem 177:229 doi:10.1016/0022-0728(84)80225-9
18. Kim YT, Collins RW, Vedam K, Allara DL (1991) J Electrochem Soc 138:3266 doi:10.1149/1.2085401
19. Salmon M, Kanazawa KK, Diaz AF, Krounbi M (1982) J Polym Sci: Polym Letts Edn 20:187
20. Otero TF, Grande H, Rodriquez J (1996) Electrochim Acta 41:1863 doi:10.1016/0013-4686(96)86826-5
21. Otero TF, Angulo E, Santamaria C, Rodriguez J (1993) Synth Met 54:217 doi:10.1016/0379-6779(93)91063-8
22. Li XG, Huang MR, Duan W, Yang YL (2002) Chem Rev 102:2925 doi:10.1021/cr010423z
23. Monk PMS, Mortimer RJ, Rosseinsky DR (2007) Electrochromism and electrochromic devices. Cambridge University Press, Cambridge
24. Reut J, Opik A, Idla K (1999) Synth Met 102:1392 doi:10.1016/S0379-6779(98)01036-4
25. Biallozor S, Kupniewska A (2005) Synth Met 155:443 doi:10.1016/j.synthmet.2005.09.002
26. Meyer H, Nichols RJ, Schroer D, Stamp L (1994) Electrochim Acta 39:1325 doi:10.1016/0013-4686(94)E0055-5
27. Inzelt G (2008) Conducting polymers:a new era in electrochemistry, Chapter 4. Springer, Berlin
28. Freund MS, Deore BA (2007) Self-doped conducting polymers, Chapter 1. Wiley, Hoboken
29. Renak ML, Bazan GC, Roitman D (1997) Adv Mater 9:392 doi:10.1002/adma.19970090505
30. Kocher C, Montali A, Smith P, Weder C (2001) Adv Funct Mater 11:31 doi:10.1002/1616-3028(200102)11:1<31::AID-ADFM31>3.0.CO;2-U
31. Gordon TJ, Yu J, Yang C, Holdcroft S (2007) Chem Mater 19:2155
32. Schirmeisen M, Beck F (1989) J Appl Electrochem 19:401 doi:10.1007/BF01015243
33. Cheung KM, Bloor D, Stevens GC (1988) Polymer (Guildf) 29:1709 doi:10.1016/0032-3861(88)90288-1
34. Kang ET, Neoh KG, Tan TC, Ong YK (1987) J Poly Sci. Part A Poly Chem 25:2143 doi:10.1002/pola.1987.080250811
35. Wynne KJ, Street GB (1985) Macromolecules 18:2361 doi:10.1021/ma00154a005

36. Cvetko BF, Brungs MP, Burford RP, Skyllas-Kazacos M (1988) J Mater Sci 23:2102 doi:10.1007/BF01115775
37. Weast RC (1987) CRC Handbook of Physics and Chemistry, 68th edn. CRC, Boca Raton
38. Li XG, Huang MR, Zhu MF, Chen YM (2004) Polymer (Guildf) 45:385 doi:10.1016/j.polymer.2003.11.014
39. Clarke TC, Scott JC, Street GB (1983) IBM J Res Develop 27:313
40. Christensen PA, Hamnett A, Hillman AR (1988) J Electroanal Chem 242:47 doi:10.1016/0022-0728(88)80238-9
41. Ivaska A, Koponen M, Passiniemi P, Osterholm JE (1989) Synth Met 28:C859 doi:10.1016/0379-6779(89)90614-0
42. Iyoda T, Aiba M, Saika T, Honda K, Shimidzu T (1991) J Chem Soc, Faraday Trans 87:1765 doi:10.1039/ft9918701765
43. Bredas JL, Street GB (1985) Acc Chem Res 18:309 doi:10.1021/ar00118a005
44. Bredas JL, Scott JC, Yakuski K, Street GB (1984) Phys Rev B Condens Matter 30:1023 doi:10.1103/PhysRevB.30.1023
45. Amemiya T, Hashimoto K, Fujishima A (1991) J Electrochem Soc 138:2845 doi:10.1149/1.2085327
46. Tian B, Zerbi G (1990) J Chem Phys 92:3892 doi:10.1063/1.457795
47. Lei J, Cai Z, Martin CR (1992) Synth Met 46:53 doi:10.1016/0379-6779(92)90318-D
48. Street GB, Clarke TC, Krounbi M, Kanazawa K, Lee V, Pfulger P, Scott JC, Weiser G (1982) Mol Cryst Liq Cryst (Phila Pa) 83:253 doi:10.1080/00268948208072174
49. Sadtler Research laboratories (1975) Sadtler Standard Spectra 13C NMR Spectra. Heyden, London
50. Warren LF, Anderson DP (1987) J Electrochem Soc 134:101 doi:10.1149/1.2100383
51. Otero TF, Ariza MJ (2003) J Phys Chem B 107:13954 doi:10.1021/jp0362842
52. Ghosh K, Maiti SN (1996) J Appl Polym Sci 60:323 doi:10.1002/(SICI)1097-4628(19960418)60:3<323::AID-APP5>3.0.CO;2-N
53. Wang Y, Yang Q, Shan G, Wang C, Du J, Wang S, Li Y, Chen X, Jing X, Wei Y (2005) Mater Lett 59:3046 doi:10.1016/j.matlet.2005.05.016
54. Cvetko BF, Brungs MP, Burford RP, Skyllas-Kazacos M (1987) J Appl Electrochem 17:1198 doi:10.1007/BF01023603
55. Wernet W, Monkenbusch M, Wegner G (1984) Makromol Chem, Rapid Commun 5:157 doi:10.1002/marc.1984.030050307
56. Yang CH, Chih YK, Tsai MS, Chen CH (2006) Electrochem Solid-State Lett 9:G49 doi:10.1149/1.2150168
57. Drury A, Chaure S, Kroll M, Nicolosi V, Chaure N, Blau WJ (2007) Chem Mater 19:4252
58. Birks LS, Friedman H (1946) J Appl Phys 17:687 doi:10.1063/1.1707771
59. Paugam L, Diawara CK, Schlumpf JP, Jaouen P, Quemeneur F (2004) Sep Purf Tech 40:237 doi:10.1016/j.seppur.2004.02.012
60. Wulfsberg G (2000) Inorganic chemisty. University Science Books, Sausalito, p 172
61. Chao TH, March J (1988) J Polym Sci Part Polym Chem 26:743 doi:10.1002/pola.1988.080260306
62. Rodriquez I, Gonzalez J (1990) J Chem Soc Chem Commun 387. doi:10.1039/c39900000387
63. Meier K, Zweifel H (1985) Radcure Europe'85 Conference, May 6–8, Basel, Switzerland, paper FC85–417